Computers, Materials & Continua
DOI:10.32604/cmc.2021.014446
Article

Tech Science Press

Timing and Classification of Patellofemoral Osteoarthritis Patients Using Fast Large Margin Classifier

Mai Ramadan Ibraheem[1], Jilan Adel[2], Alaa Eldin Balbaa[3], Shaker El-Sappagh[4], Tamer Abuhmed[5,*] and Mohammed Elmogy[6]

[1]Faculty of Computers and Information, Kafrelsheikh University, Egypt
[2]Faculty of Physical Therapy, Kafrelsheikh University, Egypt
[3]Faculty of Physical Therapy, Nahda University, NUB, Egypt
[4]Universidade de Santiago de Compostela, Santiago de Compostela, Spain
[5]College of Computing, Sungkyunkwan University, Seoul, 06351, Korea
[6]Faculty of Computers and Information, Mansoura University, Mansoura, 35516, Egypt
[*]Corresponding Author: Tamer Abuhmed. Email: tamer@skku.edu
Received: 21 September 2020; Accepted: 03 November 2020

Abstract: Surface electromyogram (sEMG) processing and classification can assist neurophysiological standardization and evaluation and provide habitational detection. The timing of muscle activation is critical in determining various medical conditions when looking at sEMG signals. Understanding muscle activation timing allows identification of muscle locations and feature validation for precise modeling. This work aims to develop a predictive model to investigate and interpret Patellofemoral (PF) osteoarthritis based on features extracted from the sEMG signal using pattern classification. To this end, sEMG signals were acquired from five core muscles over about 200 reads from healthy adult patients while they were going upstairs. Onset, offset, and time duration for the Transversus Abdominus (TrA), Vastus Medialis Obliquus (VMO), Gluteus Medius (GM), Vastus Lateralis (VL), and Multifidus Muscles (ML) were acquired to construct a classification model. The proposed classification model investigates function mapping from real-time space to a PF osteoarthritis discriminative feature space. The activation feature space of muscle timing is used to train several large margin classifiers to modulate muscle activations and account for such activation measurements. The fast large margin classifier achieved higher performance and faster convergence than support vector machines (SVMs) and other state-of-the-art classifiers. The proposed sEMG classification framework achieved an average accuracy of 98.8% after 7 s training time, improving other classification techniques in previous literature.

Keywords: Muscle activation onset time; LS-SVM; surface electromyogram; patellofemoral osteoarthritis; the timing of core muscles

1 Introduction

Biomedical signals are common electrical signals from a specified organ used to detect physical changes. These biomedical signals generally represent neuromuscular activity during constriction. The nervous system controls the contraction and relaxation activities of muscle. The muscle tissue carries electrical signals (myoelectric activity) through nerves. These electrical signals indicate potential muscle movement [1]. Muscle activity can be detected via electromyography (EMG) devices in the form of a signal [2]. The acquisition of the signal is achieved by reading EMG signals generated in the form of analog measurements. Acquiring electromyograms from active muscles is done in two ways. The electrode utilized for obtaining these muscle signals can be an invasive and non-invasive electrode [3]. sEMG is preferable in clinical and physiological applications and can be used for obtaining the desired data simply and painlessly [4]. Several problems may influence the detected surface electromyogram (sEMG) signal and, consequently, the accuracy of the detected activation timing [5]. The most obvious problem is any noise added to the EMG, resulting in significant errors in the detected EMG. Another problem is the interference of neighboring muscles in the form of crosstalk. Other problems, i.e., measurement inaccuracies, affect the final EMG signal's nature recorded [6]. Patellofemoral Pain (PFP) is a common but complex illness that affects both athletes and the general population. Functional movements are produced by contributing a chain of muscles around the hip and knee regions working in unison. The pain itself generally result from excessive increases in running mileage or the addition of strength exercises. The pain may get worse with excessive use, climbing, or going upstairs [7]. Patellofemoral Osteoarthritis (PF OA) affects the underside of the kneecap (patella) and thighbone in the (femur) that the patella rests in [8]. PF OA typically affects patients with inflammation of the joints, patellofemoral laxity, or a high-riding patella [9]. The knee joint has a complex structure with three main parts called compartments, as shown in Fig. 1. Each compartment has individual functions and structures within it. The inner compartment and the outer compartments are formed by joining the lowest part of the thighbone (femur) and the highest part of the shinbone (tibia) [10]. The inner and the outer compartment are known as medial and lateral compartments, respectively. The third compartment of the knee consists of the kneecap (patella) and the front part of the femur called the patellofemoral joint [7]. The patella protects the knee and gives control to muscles by sliding within the knee [11]. This helps shock absorption and allows the knee joint to move smoothly [12,13]. However, arthritis in the knee affects more than four million Americans annually. It is more frequently seen in women [14]. PF OA patients need progressive rehabilitation exercises in order to recover full muscle function [8]. Understanding the timing of muscle activation will guide clinicians to incorporate exercises correctly in a rehabilitation program [13]. Exercises targeting the correct musculatures will benefit patients suffering from PFP and improve their strength and motor control in these regions [9].

For a precise diagnosis of PF OA, the number of related muscle have been synchronously estimated in an experiment [8]. This research adopted the five most generic asymptomatic controls for the diagnosis of PF OA. The sEMG research tool was used for obtaining readings from the target muscles. EMG activities for the Transversus Abdominus (TrA), Vastus Medialis Obliquus (VMO), Gluteus Medius (GM), Vastus Lateralis (VL) and Multifidus Muscles (ML) were acquired for further analysis. The timing of muscle activation is an important factor in predicting joint stiffness and in measuring joint stability. Joint stability balance depends on several muscle activation values [15]. A new approach is therefore needed to distinguish sEMG signals in different patients. The proposed approach is comprised of three steps. In the pre-processing step, electromyogram signaling is enhanced to overcome the interference problems that result from neighboring muscles

in terms of crosstalk. In the second step, we extract key factor variables, i.e., burst onset, duration, and offset. Finally, a classification model is constructed using the features extracted from different patients to perform the classification task. This work aims to develop a more precise diagnostic framework for muscle activities measured using sEMG signals for PF OA patients. The order of muscle activation is determined to allow the clinician to incorporate exercises correctly in the rehabilitation program.

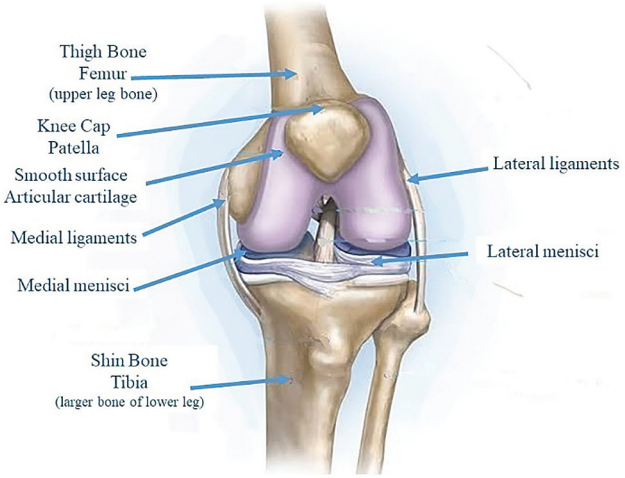

Figure 1: The knee joint structure, including the patellofemoral compartment, which is located behind the kneecap (patella)

The rest of this paper is comprised of four sections. Section 2 reviews different literature in the classification of sEMG signals. Section 3 describes electromyogram acquisition in this work and the proposed framework. Section 4 presents the classification results of the predictive model, along with discussion and comparisons. Conclusions and future work are outlined in Section 5.

2 Literature Review

Numerous studies have analyzed and classified sEMG signals acquired from the different muscles responsible for controlling different body movements. This section presents similar techniques utilized in this area, along with some of the other relevant works using different methods. For example, Cene et al. [16] proposed a classification framework based on a logistic regression algorithm to identify the sEMG signal movement. They used a gradient-descent adaptive method that was implemented to generate the proper equations for each movement. After testing their proposed logistic regression classification algorithm with the case study movement database, they achieved an average accuracy of $90.2 \pm 3.8\%$. Sadikoglu et al. [2] demonstrated a binary classification system for diagnosing a healthy individual or a neuropathy patient. The system received two different EMG signals from different patients. The results were obtained in terms of comparative figures for both healthy and neuropathy EMG signals in the time domain. Veer et al. [17] presented a classification system for sEMG signals from different upper arm muscles. They investigated muscle force relationships by applying statistical techniques for amplitude estimation. They reported an average classification accuracy of 92.50% using the ANN classifier. Khowailed et al. [18] introduced real-time muscle activity detection based on deep learning. They used a recurrent neural network (RNN) that gave the network the ability to process

time sequences. They observed a reasonable difference between the true and detected onset time. Liu et al. [19] presented an unsupervised learning framework based on a sequential Gaussian mixture model to detect EMG muscle activation. They evaluated their approach on a simulated sEMG signal whose activation was known previously. Rane et al. [20] suggested using supervised learning in building an approximate prediction model for muscular force magnitude. They evaluated their system on widely known benchmark data (International Grand Challenge Competitions) [21]. They reported the average accuracy for predicting the forces of major muscle groups as 84%. Morbidoni et al. [22] proposed an sEMG classification approach to predict foot-floor-contact during natural walking. They adopted a deep learning approach for characterizing muscular recruitment during walking. They experimented with optimization using stochastic gradient descent (SGD) and optimal learning rate. After an extensive evaluation, they achieved an average classification accuracy of 94%.

In summary, some of the previous studies focused on measuring muscle activation timing in real-time [2,18,19]. Other relevant work used different techniques for the analysis and classification of EMG signals [16,17,20,22]. The studies that measured muscle activation investigated characterizing the occurrence of active muscle from baseline in terms of the onset of muscle activation only using simulated signals [18,19]. The other EMG signal classification techniques relied on extracting statistical characteristics for the recognition process [17,22]. This work aims to develop a classification technique based on muscle activation characteristics. The proposed muscle activation-based classification model can help by giving a more precise diagnosis for PF OA patients. The extracted features can also help determine the order of muscle activation to help clinicians incorporate suitable exercises into rehabilitation programs correctly [23–26].

3 The Proposed Framework

3.1 Surface Electromyography (SEMG) Acquisition

The placement of electrodes on the muscle of interest helps in acquiring a healthy signal. The most PF OA related muscles, i.e., TrA, VMO, GM, VL, and ML, were synchronously monitored for the experiment. In this section, the steps of our muscle activation-based classification model in terms of onset, offset, and duration of muscle activation are discussed in detail. The proposed PF OA diagnosis framework consists of the following steps, as shown in Fig. 2.

For a better understanding of the sEMG signal properties, several steps, such as pre-processing, feature extraction, and classification, are required. During the first phase, several filters are applied for better separation of the signal corresponding to movements from the subject. Several possible ways to perform this pre-processing stage, rectification, and filler techniques, along with a high pass filter, were applied in this framework. Once the electromyography signal is filtered, some key feature characteristics are extracted from the signal to serve as input parameters for the classification phase. Finally, in the last stage of sEMG signal recognition, classification is implemented based on the input characteristics provided, and the classification model is constructed. The fast large margin and SVM classification algorithms were used in this work.

3.2 Signal Pre-Processing

Several problems may affect the acquired sEMG signal formation and, consequently, the accuracy of the detected activation timing [2]. The first problem is the added noise to the sEMG that results in a significant error margin in the detected EMG [27]. The second problem is the crosstalk that results from the interference of neighboring muscles. Other problems, i.e.,

measurement inaccuracies, affect the nature of the sEMG signal [28]. In the pre-processing step, electromyogram signaling is enhanced to overcome the problems mentioned above, i.e., noise and interference problems. The processing stages that are applied to the sEMG signal are summarized in the following.

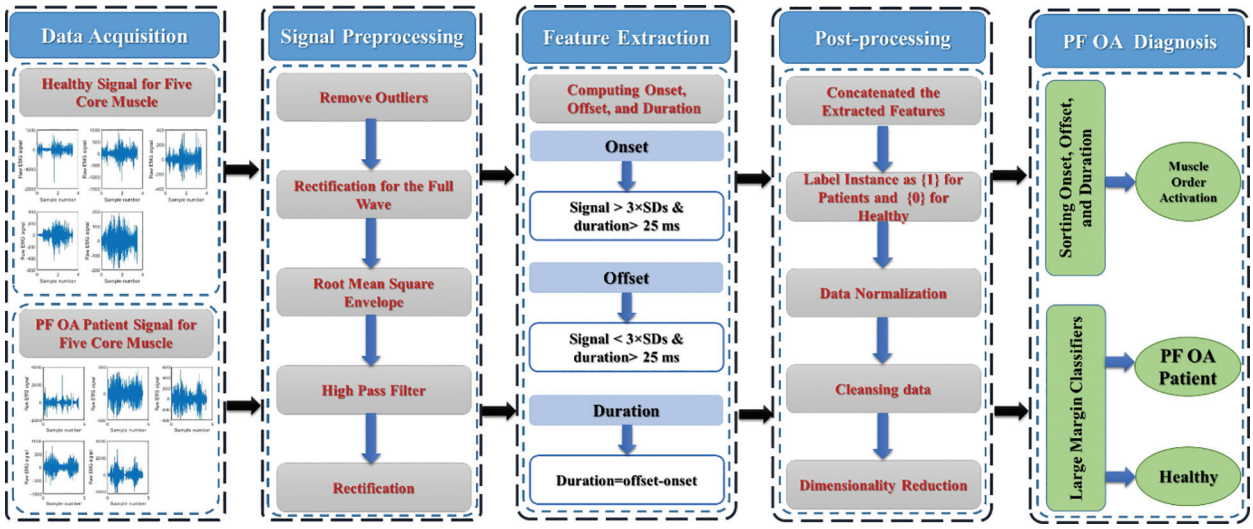

Figure 2: The PF OA diagnosis framework

3.2.1 Replace Outliers in sEMG Signal

Various background noise is received during the acquisition of the sEMG signal due to electronic equipment and other physiological factors. Proper techniques are required to eliminate noise and possible artifacts. The replace outliers method mostly finds the outliers for each of the five detected muscles and replaces them according to a filler [6]. The filler in terms of a method can be specified by each of the following ways: median, which return elements more than 3 scaled MADs (Median Absolute Deviations) from the median. mean, previous and next methods [28].

3.2.2 Rectification of the Full Wave

The sEMG signal is time and strength dependent whose amplitude takes random values above and below zero. Normalization of the sEMG signal is essential to define any characteristic properties of the signal then. The normalizing signal can be constructed by wave rectification to a scale that is common to all measurement occasions [17].

Full-wave rectification is applied by taking the absolute value of the signal. This rectification step is essential for getting a linear envelope shape for the sEMG signal [29]. Rectification turns the negative swings into positive swings. Rectification should be performed before low-passing the signal to smooth it [27]. The linear envelope of the signal can be obtained by performing filtering in both directions to eliminate any phase shift of the signal [28]. Constructing a low pass filter is also needed with order 4, and a cutoff frequency of 10 Hz. The combination of rectification and low pass filtering forms a "linear envelope" for the signal [27]. Converting the recorded sEMG signal into a linear envelope makes it easier to display and prepares it for any associated decision.

3.2.3 Root Mean Square (RMS) Envelope

When investigating the electromyogram signals detected from the surface electrode system, estimating the amplitude variation of the sEMG signal is most appropriate. The time-domain parameters in terms of RMS value can be used for identifying the proper timing of muscle activation [17]. The RMS value for the signal is plotted at the window center to avoid any envelope time shifts relative to the signal [28].

3.2.4 High Pass Filter

The number of muscle fibers, depth, amount of tissue, and location of active fibers all affect the quality of the sEMG signal recorded. These factors superimpose unwanted signals or cancel out the signal from the target muscle we are attempting to record. High-pass filtering permanently removes the effect of maintaining a constant force on or of repetitive fluctuation in the intensity from the sEMG signals [27]. A high-pass filter is well suited for eliminating the oscillation caused by superimposed artifacts. This step constructs a high pass filter using a design function with order 4, a passband frequency of 75 kHz, and a sampling frequency of 1000Hz. The designed high pass filter efficiently transforms the signals with flexible resolution in the time domain.

3.2.5 Rectification for the Final Result

The pre-processed sEMG signal is ready to be utilized in the subsequent steps of the proposed framework. Algorithm 1 shows the pre-processing steps of the proposed framework.

Algorithm 1: Pre-processing steps

Input: raw sEMG signal for the five core muscles.
Output: Enhanced sEMG signal free from any noise, offset or possible artifacts, with flexible resolution in the time domain

a. Replace Outliers in sEMG Signal using the nearest filler.
b. Rectify the Full Wave (linear envelope shape) of the sEMG signal by taking the absolute value of the signal. Then, a low pass filter is applied with order 4, and a cutoff frequency of 10 Hz.
c. Compute the Root Mean Square Envelope to estimate the amplitude variation of the sEMG signal.
d. Construct a high pass filter using a design function with order 4, a passband frequency of 75 kHz, and a sampling frequency of 1000 Hz.
e. Rectify the final result.

3.3 Feature Extraction

The temporal characteristics of specific muscle activities can be investigated by analyzing sEMG signals during movement. The recorded sEMG signals during muscle movements should mainly cover activity level (activation timing) [25]. Every group of muscles works in a sequential order to perform a specific physical activity. The timing parameters of muscular activity are signification factors in the determination of the electromechanical delay under different conditions [5]. The timing parameters can be extracted from the recorded sEMG, including onset and offset times, to identify the duration of sEMG bursts [4]. Onset and offset values are defined as follows. The time point where muscle activity begins is the onset, whereas the time point where muscle activity ends is the offset. Determination of onset and offset times enables identifying the duration

of each muscle's activity [3]. Aminaka et al. [9] defined duration as the time between muscle activation onset and offset. The detecting of timing parameters, i.e., onset, offset, and duration, also enable the determination of the order of activation for each of the five muscles. The values of onset and offset allow physicians to identify the physiological activity characteristics of the target muscle in the recorded sEMG [4]. The selection strategy is mainly based on the determination of a specific threshold value. The threshold choice lacks an agreement between the researchers [30]. Our approach adopts a threshold where the targeted muscle is considered to have reached the start time (onset) when its activity exceeds a threshold equal to three SDs above its baseline level. The activity must stay above the threshold for a minimum of 25 ms to be considered. At the same time, the muscle is considered to have reached the end time (offset) if its activity drops below the threshold equal to 3× SDs for at least a 25 ms period [31]. Algorithm 1 lists the main steps of the feature extraction stage. The proposed algorithm is used for computing muscle activation parameters, i.e., onset duration, offset duration, and order of activation. The suggested algorithm first computes SDs for each of the five involved muscle signals. Then, it checks for muscle start time (onset) where the signal value exceeds the specified threshold of 3× SDs. The signal value must exceed the specified threshold for 25 ms or more. In the same way, the algorithm checks for muscle end time (offset) where the signal value drops below the specified threshold of 3× SDs for at least 25 ms. The algorithm calculates these values for each of the five involved muscles and each signal length. Consequently, the duration can be measured by subtracting onset from offset for each muscle signal. The signal for each muscle of interest was measured several times for each patient to overcome the problem of inaccurate measurements. Net values for key feature parameters, along with their matched muscle names, are concatenated in the table below.

Algorithm 2: Feature extraction

Input: enhanced sEMG signal for the five core muscles.
Output: Obtaining onset, offset, and duration for each active muscle.
Begin For $j = 1$: no. of muscles of interest
For $i = 1$: muscle signal length
Compute SDs for each of muscles of interest;
If (signal $(i,j) > 3\times$ SDs && duration $(j) > 25$ ms)
onset $(j) = t(i)$;
If (signal $(i,j) < 3\times$ SDs && duration $(j) > 25$ ms)
offset $(j) = t(i)$;
duration = offset-onset;
For all trials:
Match column of signal with string muscle name field
mean_onset = mean(onset);
mean_offset = mean(offset);
mean_duration = mean(duration);
% Get order of activation for five-muscles
Order = sort(mean_onset);

(continued.)

```
% Save feartures extracted in to cells
net_results = {mean_onset, mean_offset, mean_duration, Order};
% Convert cell to tables then export it into CSV file
  Tableoforder = cell2table(net_results);
  writetable(Tableoforder,'order-activation.csv')
End
```

3.4 Classification

3.4.1 Post-Processing

The muscle characteristics features i.e., onset, offset, and duration are extracted for each of the five core muscles (TrA, VMO, GM, VL, and ML). The model was constructed using fifteen feature descriptors along with a labeling field to mark patients separate from healthy cases, as shown in Fig. 3.

	Transversus Abdominus			Gluteus Medius			Vastus Medialis Obliquus			Vastus Lateralis			Multifidus Muscles			Label
	Onset	Offset	Duration	Onset	Offset	Duration	Onset	Offset	Duration	Onset	Offset	Duration	Onset	Offset	Duration	Label
Patient Asc	0.026	0.032	0.282	0.038	0.859	1.56	0.566	3.478	1.8	3.478	1.534	0.534	3.196	1.762	2.619	1
Patient Dsc	0.418	0.078	0.033	1.119	0.043	3.726	3.726	1.547	3.726	1.298	3.308	3.648	1.514	2.607	1.255	1
Patient Asc	0.513	0.039	0.028	0.572	0.597	3.408	1.443	1.585	3.408	3.408	2.895	1.404	1.557	2.836	2.811	1
...	...	...	...	...	...	...	...	...	...	...	...	...	...	...	...	...
Healthy Asc	0.027	0.028	0.04	0.032	0.035	0.611	1.811	2.879	1.651	0.897	0.584	1.783	2.839	1.619	0.862	0
Healthy Asc	0.555	0.036	0.038	0.387	0.026	2.985	1.43	0.617	2.985	1.682	2.43	1.394	0.579	2.598	1.656	0
Healthy Asc	0.034	0.03	0.035	0.498	0.028	0.701	1.25	0.786	3.454	2.586	0.667	1.22	0.751	2.956	2.558	0

Figure 3: The arrangement of sEMG features fed as input to the classifier

The first row of entries in the given table shows the three discriminative features that were extracted for each of the five core muscles. The last row of entries in the table shows the three discriminative features; onset, offset, and duration, that were extracted for each muscle from healthy adults. The labeling field uses {1} to mark patients from {0} healthy cases in order to construct the training model. The extracted features are used as input data to train the linearly separable classifier. All feature matrices resulting from all trials were concatenated to form a single large matrix representing the whole dataset for the extensive margin classifiers, where each row represents a single input.

Before feeding data into the classifier, some prepossessing steps are applied to the final form of the dataset. Post-processing steps are needed to prepare, transform, and clean the data to emphasize any strong patterns in the dataset and summarize the information content. A min-max normalization for each muscle signal was performed to unify individual samples. The data cleansing helps in detecting irrelevant parts of the data, such as duplicates or coarse data. Low-quality data were removed by applying data cleansing methods. Dimensionality reduction using principal component analysis (PCA) technique is then performed to obtain the most significant

judgment variables [32]. Thus, the model was built using discriminative muscle features to evaluate the ability of the trained model to produce precise predictions. The following algorithm shows the post-processing steps.

Algorithm 3: Post-processing steps

Input: The extracted features, i.e., onset, offset, and duration for each of the five core muscles along with means of trials for each patient.
Output: The discriminative muscle features input data to train the linearly separable classifier.

a. Concatenated the extracted features in terms of the mean of muscle trials for the PF OA patients and healthy cases, where each row represented a single input.
b. Label each instance as {1} to mark patients and {0} for healthy in a labeling field.
c. Data normalization to unify data samples.
d. Cleansing data to detect and remove any irrelevant parts of the data, duplicates, or coarse data by applying data cleansing methods.
e. Dimensionality reduction using adaptive data analysis PCA technique for increasing the interpretability of the datasets while minimizing information loss.

3.4.2 Classification

Support vector machines

SVM is a machine learning algorithm for classification. The SVM's main objective is to find a dependency description between a set measured variables from an object and specific properties of these variables. Estimating the function mapping f: $RN \rightarrow \{\pm 1\}$ can be done in determining the corresponding values for new [33]. Using hard SVM, the hyperplane cannot separate in all cases. As such, in certain cases, the promotion of soft margin SVM is needed. Soft margin SVMs can find separation hyperplanes using positive slack variables, ξ_i, that can be used to adapt the constraints in Eq. (2) [34]. Slack variable adaptation gives SVM flexibility to reduce the optimization influence by allowing some cases to lie inside the margin or within the cases of another class.

$$\forall i \begin{cases} w*x_i + b \geq +1 - \xi_i & y = +1 \\ w*x_i + b \leq -1 - \xi_i & y = -1 \\ \xi_i \geq 0 \end{cases} \quad (1)$$

Fast large margin classifier

The concept of a large margin has been identified as a principle for classifying data based on the margin of classification (i.e., a scale parameter) rather than a raw training error [35]. The margin of the classification is mainly determined by locating the decision function far away from any data points [36]. Fast large margin approaches are looking to achieve large margin decision solutions by solving a constrained quadratic optimization problem and boosting with early stopping techniques [37].

The fast large margin classifier considers the above optimization and convergence techniques to reduce generalized errors and maximize the margin of separating hyperplanes. Such algorithms can save time and resources when optimizing training processes [37]. Let the quantity ρ denote the margin, the quantity which determines how well two classes can be separated and, consequently,

how fast the learning algorithm converges. Using the real-valued mapping $f: X \to R$ for classifying the pattern x; the margin can be given by Eq. (2) [35].

$$\rho_{f(x,y)} := yf(x) \tag{2}$$

Define the margin cost function $\varphi: : R \to R^+$ and φ risk of f given by Eq. (3).

$$R_\varphi(f) = E\varphi\rho_{f(x,y)} \tag{3}$$

Minimizing empirical φ risk gives Eq. (4).

$$\hat{R}_\varphi(f) = \hat{E}\varphi\rho_{f(x,y)} \tag{4}$$

The AdaBoost algorithm uses the margin cost function $\varphi(\alpha) = \exp(-\alpha)$; minimizes $\hat{R}_\varphi(f)$ using greedy basis selection, line search [35].

Classifiers should achieve a large margin ρ_f for reliable training and also to perform well on unseen instances. These algorithms can perform training more robustly concerning patterns and parameters. The maximum margin hyperplanes f^* can be given by Eq. (5) [35].

$$f^* := \arg\max_f \rho_f : = \operatorname{argmax}_f \min_i y_i f(x_i) \tag{5}$$

The maximum margin f for the optimal hyperplane can be given such that the weight vector and threshold satisfy Eq. (6).

$$w^*, b^* = \arg\max_{w,b} \sum_{i=1}^{m} \min \frac{(w \cdot x_i) + b}{\|w\|} \tag{6}$$

The maxi–min optimization problem can be transformed into a constrained optimization task by maximizing the subject to the margin lower bound ρ as in Eq. (7) [35].

$$w^*, b^*, \rho^* = \arg\max_{w,b,\rho} \rho \ \textit{subject to} \ \frac{(w \cdot x_i) + b}{\|w\|} \geq \rho \quad \textit{for} \ 1 \leq i \leq m \tag{7}$$

$$w^*, b^*, \rho^* = \arg\max_{w,b,\rho} \rho \ \textit{subject to} \ \|w\| = 1 \ \textit{and} \ y_i((w \cdot x_i) + b) \geq \rho \quad \textit{for} \ 1 \leq i \leq m$$

High noise cases result in a significant overlap within the classes. The previous maximum margin algorithms perform poorly in this case because the maximum-minimum margin achieves negative values. A standard approach to overcome the sensitivity to noisy training patterns is by introducing slack variables (Eq. (8)). The relaxed constraints take the form of Eq. (9) [36].

$$\xi_i \geq 0, \quad \textit{for all} \ i = 1, \ldots, m \tag{8}$$

$$y_i((w \cdot x_i) + b) \geq 1 - \xi_i, \quad \textit{for all} \ i = 1, \ldots, m \tag{9}$$

By controlling both the size of w and the number of training errors, we can minimize the following objective function, where the constant $C > 0$, a classifier that generalizes well, can then be found by Eq. (10) [35].

$$\tau(w, \xi) = \frac{1}{2}\|w\|^2 + C\sum_{i=1}^{m} \xi_i \tag{10}$$

Incorporating kernels k for the dot products $k(x, x_i)$ and Lagrange multipliers α_i, subject to the constraints leading to decision functions of the more general form.

$$f(x) = \sum_{i=1} \alpha_i k(x, x_i) + b \tag{11}$$

A fast large margin algorithm has several advantages. First, it converges in a finite number of updates. Second, the solution is optimized to give the maximum possible margin [35]. Experimental results using a fast large margin algorithm show higher performance and faster convergence compared to SVMs and other state-of-the-art classifiers.

4 Experimental Results

4.1 Dataset

The dataset was synchronously captured form five PF OA related muscles: TrA, VMO, GM, VL, and ML. The data from the five muscles were acquired for each activity, such as going upstairs. The dataset was acquired at the Outpatient Clinic, Faculty of Physical Therapy, Cairo University using quantitative EMG with surface electrodes. The sEMG data signal of the dataset was recorded at the Department of Biomedical Engineering, Faculty of Engineering, Cairo University.

This dataset has a total of 186 records for PF OA patients and 66 records for healthy individuals. This dataset is comprised of training cases along with corresponding clinical label diagnosis cases. Different pre-processing steps, i.e., normalization, cleansing, and dimensionality reduction, were performed to prepare the data to be fed into the classifier. Different evaluation metrics were adopted to check the significance of the proposed PF OA diagnosis framework.

4.2 Performance Evaluation

The four outcomes of positive instances (P) and negative instances (N) formulates a 2×2 confusion matrix for the experiment. The area under the ROC (receiver operating characteristics) curve (AUC) is an important evaluation metric for checking the performance of the classification model. The ROC curve is plotted with the TPR (True Positive Rate) against the FPR (False Positive Rate), where TPR is on the y-axis, and FPR is on the x-axis [38]. The accuracy (ACC) measure is used to check the capability of the classification model. Accuracy can be calculated using Eq. (12). The sensitivity (Sen.) or recall measure is used to check the capability of our classifier to recognize the positive class patterns. The Sen of the classifier can be determined using Eq. (13). The specificity (Spec.) measure is used to check the capability of the classifier to recognize the negative class patterns. It can be calculated using Eq. (14). The F-measure or dice similarity coefficient (DSC) considers both precision and recall to measure the accuracy of the test. DSC ranges from 0, the worst score, to 1, the best score, as a weighted average of precision and recall. The DSC measure can be calculated using Eq. (15) [39].

$$\text{Accuracy} = \frac{\text{TP} + \text{TN}}{(\text{TP} + \text{FP} + \text{TN} + \text{FN})} \times 100 \tag{12}$$

$$\text{Sen.} = \frac{\text{TP}}{\text{TP} + \text{TN}} \tag{13}$$

$$\text{Spec.} = \frac{\text{TN}}{\text{TN} + \text{FP}} \tag{14}$$

$$\text{DSC} = 2 \times \frac{\text{Precision} \times \text{Recall}}{\text{Precision} + \text{Recall}} \tag{15}$$

4.3 Results

Large margin classifiers were used to evaluate the performance of the proposed model, i.e., fast large margin and SVM classifiers. Significant evaluation metrics were used to check the capability of the model at distinguishing between classes. ACC, AUC, DSC, Sen, and Spec are used as performance indicators. These evaluation metrics are considered along with total time spent in training to indicate the convergence rate. The proposed framework achieved higher performance results using the fast large margin and SVM classifiers. The higher performance from using the fast large margin classifier was achieved in shorter computing time than with SVM. The proposed system achieved an average ACC equal to 98.8%, AUC equal to 0.999, DSC equal to 99.1%, Sen equal to 99.9%, and Spec equal to 96.0% in 7 s using the fast large margin classifier and an average ACC equal to 98.8%, AUC equal to 0.999, DSC equal to 99.1%, Sen equal to 99.9%, and Spec equal to 96.0% using the SVM classifier in 21 s.

To evaluate the results of the proposed system, the computed results were compared with other state-of-the-art classifiers. These classifiers are the generalized linear model (GLM), logistic regression, Naïve Bayes, deep learning, decision trees, random forest, and gradient boosted trees (GBT). The comparison measurements are listed in Tab. 1, as follows GLM, logistic regression, Naïve Bayes, deep learning, decision trees, random forest, and GBT achieved ACC equal to 97.4%, 96.1%, 97.4%, 96.1%, 80.6%, 79.3%, and 91.0%, respectively. They achieved average AUC equal to 0.996, 0.992, 0.996, 0.999, 0.689, 0.943 and 0.732, respectively. They achieved average DSC equal to 98.2%, 97.4%, 98.2%, 97.3%, 88.0%, 83.4%, and 94.0%, respectively. They achieved average Sen equal to 99.9%, 99.9%, 98.5%, 98.0%, 96.9%, 72.3%, and 96.9%, respectively. They achieved average Spec equal to 92.0%, 82.0%, 96.0%, 89.3%, 36.7%, 99.9%, and 74.0%, respectively. The training time of these classifiers was 3, 4, 7, 7, 7, 38, and 125 s, respectively. The proposed system, using the fast large margin and SVM classifiers, outperformed the other state-of-the-art techniques in terms of accuracy. When it comes to convergence time, the fast large margin classifier outperforms SVM and the other tested classifiers in the comparative evaluation.

Table 1: The performance evaluation of the proposed technique with other classifiers

Model	ACC. (%)	AUC	DC (%)	Sen. (%)	Spec. (%)	Total time (s)
GLM	97.4	0.996	98.2	99.9	92.0	3
Logistic regression	96.1	0.992	97.4	99.9	82.0	4
Naïve Bayes	97.4	0.996	98.2	98.5	96.0	7
Deep learning	96.1	0.999	97.3	98.0	89.3	7
Decision trees	80.6	0.689	88.0	96.9	36.7	7
Random forest	79.3	0.943	83.4	72.3	99.9	38
GBT	91.0	0.732	94.0	96.9	74.0	125
SVM	98.8	0.999	99.1	99.9	96.0	21
Fast large margin	98.8	0.999	99.1	99.9	96.0	7

The convergence and robustness are illustrated by the training time in seconds, as shown in Tab. 1. To visualize the performance of the proposed model, the ROC curve was constructed along with the other comparative classifiers. The ROC curve was created by plotting the TPR against the FPR. Fig. 4 shows the relationship between Sen and Spec for all comparative techniques. The results show the superiority of the proposed framework's predictions *vs.* the other techniques.

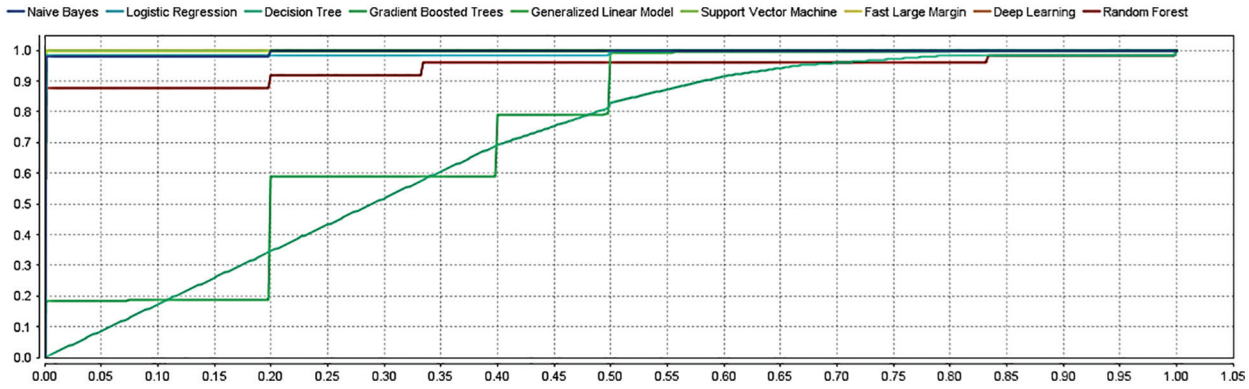

Figure 4: The ROC curve for the tested classifiers

4.4 Discussion

sEMG based research considered in the comparison can be divided into two major categories. Some of them investigated measuring muscle activity, and other relevant work explored the classification of EMG signals using various approaches. Khowailed et al. [18] and Liu [19] investigated measuring muscle activation and characterized the active muscles from their baseline state in terms of the onset of muscle activation. Other sEMG based techniques are concerned with the analysis and classification of EMG signals [2,16,17,20,22]. Most EMG signal classification techniques are based on real time-domain features. The classification studies in recent literature have been carried out based on extracting statistical characteristics for the recognition process [17,22].

To provide a comparison with feature-based methods, a classification technique based on muscle activation characteristics was developed. The proposed classification model investigates extracting core muscle activation in terms of onset, offset, and duration of muscle activation for a more precise diagnosis for PF OA arthritis patients. The extracted feature space is used to construct the classification model. Large margin classifiers were used for training the model to discriminate the labeled PF OA arthritis patients *vs.* healthy cases. The fast large margin classifier utilized the LS-SVM solver type in this method. The penalty parameter of the error term was $C = 10$, the tolerance of the termination criterion ξ, class weights w, intercept value bias was set as optimal parameters. The penalty parameter values over the training processes, along with error terms, are given in Tab. 2. It can be seen that the optimal penalty parameter value over the training processes is 10, which corresponds to the smallest error shown in Fig. 5.

Several comparative classifiers converged in a short time but with lower performance, i.e., logistic regression, Naïve Bayes, deep learning, and decision trees. The proposed fast large margin classifier achieves higher accuracy in shorter convergence time, as shown in Fig. 5.

Table 2: The penalty parameter values over the training processes along with error terms

C	Error rate (%)
0.001	13.7
0.010	23.8
0.100	8.1
1	5.0
10	2.5
100	2.5
1000	6.3

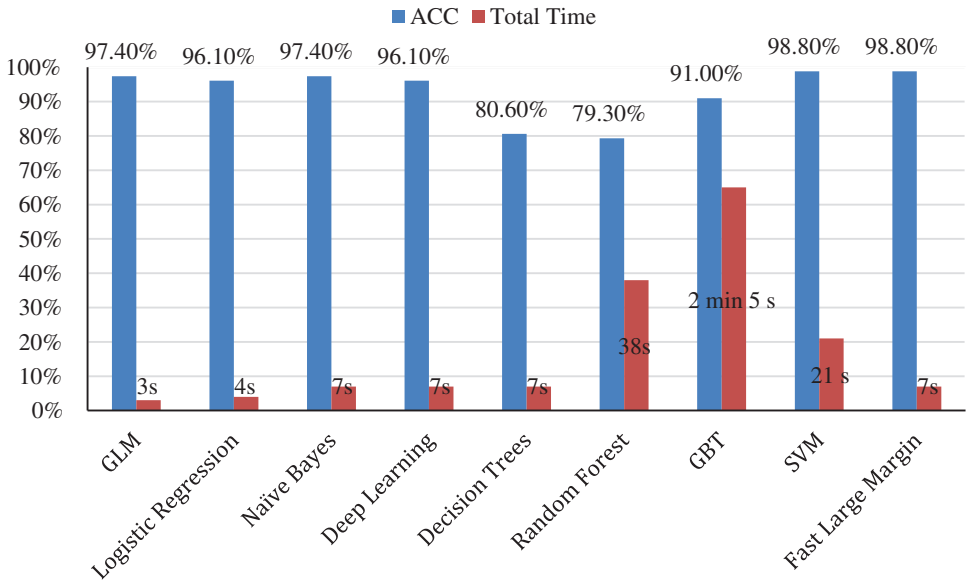

Figure 5: Comparison in terms of accuracy with convergence time

Some of the previous studies evaluated their approach using a real-time domain comparison [2,18,19]. Other studies on classification techniques evaluated their work in terms of accuracy. Cene et al. [16] proposed a classification framework based on a logistic regression algorithm to identify the sEMG signal movement. Their system achieved an average accuracy equal to 90.2%. Veer et al. [17] introduced a classification model that discriminated against the strength of the movement as high or low from the sEMG signal. The model was trained using an ANN with pre-defined arm motions and achieved an average classification accuracy of 92.5%. Rane et al. [20] proposed a supervised model for predicting muscular force-based EMG movement signals as inputs to a hierarchical model. Their system achieved an average accuracy equal to 84%. Morbidoni et al. [22] proposed a deep learning approach to predict foot-floor-contact during natural walking for sEMG signals. The sEMG signals were acquired from eight lower-limb muscles of 23 healthy subjects during walking, and the model achieved an average classification accuracy of 94%.The proposed fast large margin classification model based on muscle activation features extracted is compared with the sEMG signal feature-based classification techniques in the literature. The proposed fast large margin classification model based muscle activation features achieved

98.8% classification accuracy. The presented model uses muscle activity timing as a feature space, while others carried out a classification task based on statistical characteristics. The extracted feature space can also help in determining the order of muscle activation to help clinicians to incorporate suitable exercises into a rehabilitation program correctly. The results of the proposed model were evaluated using the acquired sEMG signals from PF OA arthritis patients *vs.* healthy cases. However, in some studies, the experiments were carried out using a simulated signal. The implemented framework shows promising results in sEMG signal analysis since the accuracy rate outperforms other studies with similar techniques in this area. The trained fast large margin classifier allows the system to automatically learn relevant features and determine the modification of muscular activation patterns to compensate for the muscle disorders efficiently. The proposed PF OA arthritis classification model provides novel insights to approximate the accurate timing of core muscles in designing treatment exercises.

5 Conclusion

This work proposed a precise diagnosing approach for PF OA arthritis patients. The developed predictive model investigates PF OA arthritis muscle timing features. sEMG signals were acquired from five core muscles over 252 reads from PF OA patients and healthy adults while stepping upstairs. Onset, offset, and duration times for TrA, VMO, GM, VL, and ML muscles were acquired to construct the classification model. PF OA arthritis muscle timing features were extracted using function mapping from real-time space to a PF OA arthritis discriminative feature space. The extracted features helped determine the order of muscle activation for a clinician to incorporate suitable exercises into a rehabilitation program correctly. The fast large margin classifier results based on the muscle timing activation features achieved higher performance and faster convergence than SVM and other state-of-the-art classifiers. The implemented framework shows promising results in sEMG signal analysis since the accuracy rate outperforms other similar techniques in this area. In future work, more analysis of the signal and expanding the dataset is required. Hierarchical networks can also be used for deep training.

Funding Statement: This work was supported by the National Research Foundation of Korea (NRF) Grant funded by the Korean government (MSIT) (NRF-2016R1D1A1A03934816) and by Chowis Co., Ltd.

Conflicts of Interest: The authors declare that they have no conflicts of interest to report regarding the present study.

References

[1] J. Rodriguez-Falces, J. Navallas and A. Mal, "EMG modeling," in *Computational Intelligence in Electromyography Analysis-A Perspective on Current Applications and Future Challenges*, London, UK: IntechOpen, 2012.

[2] F. Sadikoglu, C. Kavalcioglu and B. Dagman, "Electromyogram (EMG) signal detection, classification of EMG signals and diagnosis of neuropathy muscle disease," *Procedia Computer Science,* vol. 120*,* pp. 422–429, 2017.

[3] A. Mika, B. C. Clark and L. Oleksy, "The influence of high and low heeled shoes on EMG timing characteristics of the lumbar and hip extensor complex during trunk forward flexion and return task," *Manual Therapy,* vol. 18*,* no. 6*,* pp. 506–511, 2013.

[4] U. Rashid, I. K. Niazi, N. Signal, D. Farina and D. Taylor, "Optimal automatic detection of muscle activation intervals," *Journal of Electromyography and Kinesiology,* vol. 48*,* pp. 103–111, 2019.

[5] G. Staude, C. Flachenecker, M. Daumer and W. Wolf, "Onset detection in surface electromyographic signals: A systematic comparison of methods," *EURASIP Journal on Advances in Signal Processing,* vol. 2001, no. 2, pp. 67–81, 2001.

[6] K. Veer and R. Agarwal, "Wavelet denoising and evaluation of electromyogram signal using statistical algorithm," *International Journal of Biomedical Engineering and Technology,* vol. 16, no. 4, pp. 293, 2014.

[7] R. Becker, M. Röpke, A. Krull, V. Musahl and W. Nebelung, "Surgical treatment of isolated patellofemoral osteoarthritis," *Clinical Orthopaedics and Related Research,* vol. 466, no. 2, pp. 443–449, 2008.

[8] J. Kiel and K. Kaiser, "Patellofemoral arthritis," in *Treasure Island*, FL, USA: StatPearls, PMID, 2019.

[9] N. Aminaka, B. G. Pietrosimone, C. W. Armstrong, A. Meszaros and P. A. Gribble, "Patellofemoral pain syndrome alters neuromuscular control and kinetics during stair ambulation," *Journal of Electromyography and Kinesiology,* vol. 21, no. 4, pp. 645–651, 2011.

[10] H.-P. W. Van Jonbergen, R. W. Poolman and A. Van Kampen, "Isolated patellofemoral osteoarthritis," *Acta Orthopaedica,* vol. 81, no. 2, pp. 199–205, 2010.

[11] C. Eapen, C. D. Nayak and C. P. Zulfeequer, "Effect of eccentric isotonic quadriceps muscle exercises on patellofemoral pain syndrome: An exploratory pilot study," *Asian Journal of Sports Medicine,* vol. 2, no. 4, pp. 227–234, 2011.

[12] N. Wyndow, N. Collins, B. Vicenzino, K. Tucker and K. Crossley, "Is there a biomechanical link between patellofemoral pain and osteoarthritis? A narrative review," *Sports Medicine,* vol. 46, no. 12, pp. 1797–1808, 2016.

[13] X. Xu, C. Yao, R. Wu, W. Yan, Y. Yao *et al.,* "Prevalence of patellofemoral pain and knee pain in the general population of Chinese young adults: A community-based questionnaire survey," *BMC Musculoskeletal Disorders,* vol. 19, no. 1, pp. 165–171, 2018.

[14] J. D. Willson, T. W. Kernozek, R. L. Arndt, D. A. Reznichek and J. S. Straker, "Gluteal muscle activation during running in females with and without patellofemoral pain syndrome," *Clinical Biomechanics,* vol. 26, no. 7, pp. 735–740, 2011.

[15] A. Motealleh, N. Maroufi, J. Sarrafzadeh, M. A. Sanjari and N. Salehi, "Comparative evaluation of core and knee extensor mechanism muscle activation patterns in a stair stepping task in healthy controls and patellofemoral pain patients," *Journal of Rehabilitation Sciences & Research,* vol. 1, no. 4, pp. 84–91, 2014.

[16] V. H. Cene and A. Balbinot, "Upper-limb movement classification through logistic regression sEMG signal processing," in *Latin America Congress on Computational Intelligence (LA-CCI),* Curitiba, Brazil: IEEE, pp. 1–5, 2015.

[17] K. Veer and T. Sharma, "Extraction and Analysis of above elbow SEMG for Pattern classification," *Journal of Medical Engineering & Technology,* vol. 40, no. 4, pp. 149–154, 2016.

[18] I. A. Khowailed and A. Abotabl, "Neural muscle activation detection: A deep learning approach using surface electromyography," *Journal of Biomechanics,* vol. 95, pp. 109322, 2019.

[19] J. Liu, D. Ying, W. Z. Rymer and P. Zhou, "Robust muscle activity onset detection using an unsupervised electromyogram learning framework," *PLoS ONE,* vol. 10, no. 6, pp. e0127990, 2015.

[20] L. Rane, Z. Ding, A. H. McGregor and A. M. J. Bull, "Deep learning for musculoskeletal force prediction," *Annals of Biomedical Engineering,* vol. 47, no. 3, pp. 778–789, 2018.

[21] A. L. Kinney, T. F. Besier, D. D. DtextquotesingleLima and B. J. Fregly, "Update on grand challenge competition to predict in vivo knee loads," *Journal of Biomechanical Engineering,* vol. 135, no. 2, pp. 131, 2013.

[22] S. F. A. Cucchiarelli, C. Morbidoni and F. D. Nardo, "A deep learning approach to emg-based classification of gait phases during level ground walking," *Electronics,* vol. 8, no. 8, pp. 894, 2019.

[23] K. M. Park, S. Y. Kim and D. W. Oh, "Effects of the pelvic compression belt on gluteus medius, quadratus lumborum, and lumbar multifidus activities during side-lying hip abduction," *Journal of Electromyography and Kinesiology,* vol. 20, no. 6, pp. 1141–1145, 2010.

[24] E. Kellis and V. Kouvelioti, "Agonist versus antagonist muscle fatigue effects on thigh muscle activity and vertical ground reaction during drop landing," *Journal of Electromyography and Kinesiology,* vol. 19, no. 1, pp. 55–64, 2009.

[25] S. Boudreau, D. Farina, L. Kongstad, D. Buus, J. Redder *et al.,* "The relative timing of trunk muscle activation is retained in response to unanticipated postural-perturbations during acute low back pain," *Experimental Brain Research,* vol. 210, no. 2, pp. 259–267, 2011.

[26] P. Marshall and B. Murphy, "The validity and reliability of surface EMG to assess the neuromuscular response of the abdominal muscles to rapid limb movement," *Journal of Electromyography and Kinesiology,* vol. 13, no. 5, pp. 477–489, 2003.

[27] R. Chowdhury, M. Reaz, M. Ali, A. Bakar, K. Chellappan *et al.,* "Surface electromyography signal processing and classification techniques," *Sensors,* vol. 13, no. 9, pp. 12431–12466, 2013.

[28] A. Mengarelli, S. Cardarelli, F. Verdini, L. Burattini, S. Fioretti *et al.,* "A matlab-based graphical user interface for the identification of muscular activations from surface electromyography signals," in *38th Annual Int. Conf. of the IEEE Engineering in Medicine and Biology Society (EMBC)*, pp. 3646–3649, 2016.

[29] O. Barzilay and A. Wolf, "A fast implementation for EMG signal linear envelope computation," *Journal of Electromyography and Kinesiology,* vol. 21, no. 4, pp. 678–682, 2011.

[30] K. T. Ozgunen, U. Celik and S. S. Kurdak, "Determination of an optimal threshold value for muscle activity detection in EMG analysis," *Journal of Sports Science & Medicine,* vol. 9, no. 4, pp. 620, 2010.

[31] L. Cavazzuti, A. Merlo, F. Orlandi and I. Campanini, "Delayed onset of electromyographic activity of vastus medialis obliquus relative to vastus lateralis in subjects with patellofemoral pain syndrome," *Gait & Posture,* vol. 32, no. 3, pp. 290–295, 2010.

[32] I. T. Jolliffe and J. Cadima, "Principal component analysis: A review and recent developments," *Philosophical Transactions of the Royal Society A: Mathematical, Physical and Engineering Sciences,* vol. 374, no. 2065, pp. 20150202, 2016.

[33] T. N. Hui Cao and Y. Ninomiya, "Approximate RBF kernel SVM and its applications in pedestrian classification," in *Int. Workshop on Machine Learning for Vision-Based Motion Analysis*, Marseille, France, 2008.

[34] J. Cervantes, F. Garcia-Lamont, L. Rodriguez-Mazahua and A. Lopez, "A comprehensive survey on support vector machine classification: Applications, challenges and trends," *Neurocomputing,* vol. 408, pp. 189–215, 2020.

[35] A. J. Smola, P. Bartlett and D. Schuurmans, "*Advances in large margin classifiers*," Cambridge, MA, USA: MIT Press, 2000.

[36] H. Panwar and S. Gupta, "Optimized large margin classifier based on perceptron," in *Advances in Intelligent and Soft Computing,* Heidelberg, Berlin: Springer, pp. 385–392, 2012.

[37] Y. Wei, F. Yang and M. J. Wainwright, "Early stopping for kernel boosting algorithms: A general analysis with localized complexities," *IEEE Transactions on Information Theory,* vol. 65, no. 10, pp. 6685–6703, 2019.

[38] A. P. Bradley, "The use of the area under the ROC curve in the evaluation of machine learning algorithms," *Pattern Recognition,* vol. 30, no. 7, pp. 1145–1159, 1997.

[39] M. R. Ibraheem and M. Elmogy, "Automated segmentation and classification of hepatocellular carcinoma using fuzzy c-means and SVM," *Medical Imaging in Clinical Applications,* vol. 651, pp. 193–210, 2016.